One-step elaboration of Janus polymeric nanoparticles: A comparative study of different emulsification processes

Madeline Vauthier, Marc Schmutz, Christophe Serra

One-step Elaboration of Janus Polymeric Nanoparticles: a Comparative Study of Different Emulsification Processes

Madeline Vauthier,†* Marc Schmutz†, Christophe Alexandre Serra†

† Université de Strasbourg, CNRS, Institut Charles Sadron UPR 22, F-67000 Strasbourg, France
Email: madeline.vauthier@ics-cnrs.unistra.fr, marc.schmutz@ics-cnrs.unistra.fr, ca.serra@unistra.fr
Corresponding author: Dr. M. Vauthier, +33(0)388 414 194

ABSTRACT:
Hypothesis:
Janus polymeric nanoparticles have attracted much attention for their wide range of applications in various fields due to the presence of two domains with different chemistries, compositions or functionalities. This type of particles is obtained by various conventional methods which require several steps (the particle elaboration and the surface functionalization), sometimes leading to the elaboration of emulsions with large and multimodal sizes distributions. Various physical and chemical parameters influence the particles size, morphology and stability.
Experiments
In this study, we propose to prepare polymeric Janus nanoparticles (JNPs) by a one-step method from a mixture of two different polymers and to compare several emulsification-evaporation processes (sonication, shear mixing and elongational-flow micromixing).
Findings
The possibility to obtain monomodal JNPs (diameter lower than 200 nm) with a hydrophobic domain (poly(lactic-co-glycolic acid), PLGA) and a hydrophilic charged domain (based on poly(styrene sulfonate), PSS) was demonstrated only with the elongational-flow micromixer.

KEY WORDS: Janus nanoparticles, biocompatible polymer, emulsification, elongational-flow micromixer, poly(lactic-co-glycolic acid), poly(styrene sulfonate), interfacial chemistry

I. INTRODUCTION

Particles having biphasic geometry of various composition and properties are called "Janus particles",[1,2] inspired by the eponym two-faced Roman god. This anisotropic nature gives rise to unique properties, which made these particles very useful in a wide range of applications, such as biosensing,[3,4] theranostics,[5,6] smart textiles[7] or dielectrophoresis[8,9]. A well-known example is the bicolored Janus microparticles with electrical anisotropy realized by Torii's group thanks to a 2D microfluidic technology.[10] They generated precursor Janus droplets subsequently cured into monodispersed bicolored polymeric Janus particles. Although various processes such as toposelective surface modification (partially masked particles,[11] using reactive directional fluxes,[12,13] microcontact printing[14,15] or partial contact with reactive media[16]), template-directed self-assembly of particles,[17] controlled phase separation phenomena[18,19] or controlled surface nucleation[20] have been studied for the fabrication of Janus-like particles. However, difficulties in scaling up the productivity prevented the widespread use of these techniques. Moreover, most of these fabrication methods need several steps: the particles' formation and the surface functionalization[21] and/or are very tricky to control. Nowadays, beside the microflu-

idic route developed by Torri and coll., there is only one method allowing quite easily the one-step formation of Janus microparticles (around 100 µm): the dual-supplied spinning disk technique. Two different polymer solutions of two different colors are introduced on opposite sides of a spinning disk where they flow to the edge and form jets which have two different colors. Due to the Rayleigh instability, they form bichromatic droplets which solidify in the air. This technique is used, for example, in the Gyricon display medium[22] and for biological images.[23] However, if the desired application is to further deliver drugs by intravenous injection, it is crucial to have nanoscale particles (diameter lower than 1 µm),[24–26] with a hydrophilic and/or charged surface to favor the cells penetration.[27–29]

The original approach of this study was based on the combination of the emulsification-evaporation method and the use of a various emulsification devices. Contrary to previous studies that started from monomers and thus required a polymerization step,[21] two different polymers were directly introduced in the devices. To the best of our knowledge, there is no one-step method described in the literature that allows the formation of composite polymeric Janus nanoparticles. In the present study, we compare different emulsification-evaporation methods (sonication, shear mixing and elongational-flow micromixing) in order to elaborate one-step composite polymeric Janus nanoparticles (JNPs). Because process and physical-chemistry parameters highly influence the NPs size, these various parameters are also varied in order to achieve the elaboration of the smallest and the more monomodal JNPs.

II. MATERIALS AND METHODS

II.1. Materials

Poly(lactic-co-glycolic acid) 50:50 (PLGA) (Resomer® RG504 H, Sigma, 50,000 $g.mol^{-1}$), poly(styrene sulfonate) (PSS) (Sigma, 70,000 $g.mol^{-1}$), ethyl acetate (Sigma), sodium dodecyl sulfate (SDS) (92.5%, Sigma) as an ionic surfactant and Pluronic® F-127 (Sigma) as a non-ionic surfactant were used as received to prepare the nanosuspensions.

The continuous phase was composed of 15 $g.L^{-1}$ of surfactant (Pluronic® F-127 or SDS) solubilized in deionized water. The dispersed phases were composed of 1w% of polymer(s) solubilized in ethyl acetate. Since the continuous/dispersed phase (C/D) volume ratio may influence a lot the particles' size, this parameter was changed in the presented study. The x value (x=w% of PSS/w% of PLGA) was modified in order to change the solution's composition and viscosity.

II.2. Preparation of nanosuspensions by ultrasonication

Nanosuspensions were first performed with an ultrasonic processor (450W, SONOPULS UW 2200, Bandelin) used at a given processing cycle (t_{on}/t_{total}) and a frequency of 20 kHz. This device formed nanoemulsions, nanodroplets of both polymers and solvent dispersed in the continuous phase, due to bubbles implosion. The continuous phase and the dispersed phase, for a total volume of 5 mL, were introduced in a plastic vial before being sonicated for a given time. At the end of the operation, the samples were left overnight in a fume hood to let the polymers' solvent evaporated resulting in the final obtention of a suspension of composite polymeric nanoparticles (nanosuspension).

II.3. Preparation of nanosuspensions by shear mixing

The rotor-stator mixer (Ultra-Turrax® T25 basic, IKA®-Werke) allowed the formation of nanoemulsions by shearing the two phases. In this study, the continuous and the dispersed phases, for a total volume of 15 mL, were introduced in a plastic vial before being mixed with the rotor-stator mixer at 800W for a given time at a given speed. At the end of the operation, the samples were left overnight in a fume hood to let the polymers' solvent evaporated.

II.4. Preparation of nanosuspensions by elongational-flow micromixing

The continuous phase and the dispersed phase (total volume of 10 mL) were used as the raw material for the system. As illustrated in Figure 1, the emulsification system was mainly assembled with two mid-pressure sy-

ringe pumps (neMESYS® Mid Pressure Module, Cetoni) which can work in opposite phase (withdraw/infuse), two 25 mL stainless steel syringes (Cetoni) and one PEEK tee (Valco Vici). The system was controlled by the supplier's software to precisely operate flow rate. The three drilled cylindrical microchannels have a diameter of 150 µm. Two microchannels were connected to the syringes with two PTFE tubes (1.06 mm ID x 1.68 mm OD). The third microchannel was used to collect the emulsion. During the process, both pumps were operated in opposite phases at the same reciprocating flow rate so that the premixed emulsions were transferred from one syringe to the other one through the microchannels, acting as a restriction to the flow, forming nanoemulsions by elongational droplet rupture. A back and forth movement of the pump counts for one cycle. At the end of the operation, the samples were collected, poured in a vial and left overnight in a fume hood to let the polymers' solvent evaporated.

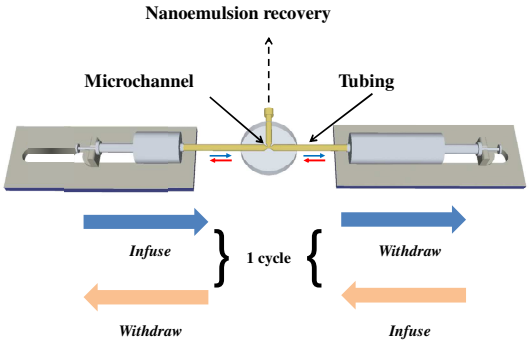

Figure 1. Schematic illustration of the elongational-flow micromixing device.

II.5. Characterization methods

II.5.1. Diameter, size distribution and zeta potential

The z-average diameter, size distribution and zeta potential of the nanoparticles were assessed by dynamic light scattering (DLS) using a Malvern Nano ZetaSizer instrument (Malvern, Orsay, France). The helium-neon laser (4 mW) was operated at 633 nm, the scatter angle was fixed at 173° and the sample temperature was maintained at 25°C.

The polydispersity index of the particle size (PDI) is a measure of the broadness of the size distribution and it is commonly admitted that PDI values below 0.2 corresponds to monomodal distributions.[30–32] Analyses of nanosuspensions size and zeta potential were performed by pouring dropwise 0.02 mL of the nanosuspensions into 1 mL deionized water. Measurements were conducted in triplicates, each measurement being an average of 30 values calculated by the ZetaSizer.

II.5.2. Transmission Electron Microscopy

To analyze the morphology and shape of the composite nanoparticles, cryo-transmission electron microscopy (cryo-TEM) experiments were performed. A 5 µL drop of the NPs suspension was deposited onto a lacey-holey carbon film (Ted Pella) freshly glow discharged (Elmo, Cordouan Technologies). The grid was rapidly frozen in liquid ethane cooled by liquid nitrogen in a home-made environment-controlled machine. The grids were mounted onto a Gatan 626 cryoholder and observed in a Tecnai G2 (FEI-Eindhoven) operating at 200 kV and the images were taken with an Eagle 2k2k ssCCD camera (FEI- Eindhoven) under low dose conditions. The contrast was, in that case, directly related to the atomic number of the diffusing atoms.

II.5.3. Viscosity measurements

The viscosity of the different phases was measured at 25°C by means of an Ostwald viscometer (Categorie I). This method was based on the determination of the time required for the solution to flow through a capillary. Each measurement was repeated four times and a mean value for the flow time was taken. This time was then correlated to the kinematic viscosity $\nu = K (t-H)$. K was a constant related to the capillary (equal to 0.01 $mm^2.s^{-2}$ in our case), t was the average flow time (s) and H was the Hagenbach correction of time (here, H = 0 s).

The values of the dispersed and continuous phase dynamic viscosities, respectively η_d and η_c, were then easily determined from their respective density since $\eta = \rho\nu$.

III. RESULTS AND DISCUSSIONS

III.1. Formation of polymeric nanoparticles

In this first part, the possible formation of polymeric nanoparticles (NPs) with 1w% PSS or 1w% PLGA-based dispersed phase was investigated. In this purpose the mixing parameters (MP), the emulsification times and the C/D volume ratio were varied as indicated in Table 1. 0.3w% of non-ionic surfactant (Pluronic® F-127) was used, otherwise notified.

III.1.1. Variation of the processes' mixing parameter (MP)

The emulsification times were fixed at the following values:

- Ultrasonication: 5 min of emulsification
- Rotor-stator mixer: 10 min of shear mixing
- Elongational-flow micromixer: 80 min (100 cycles)

a)

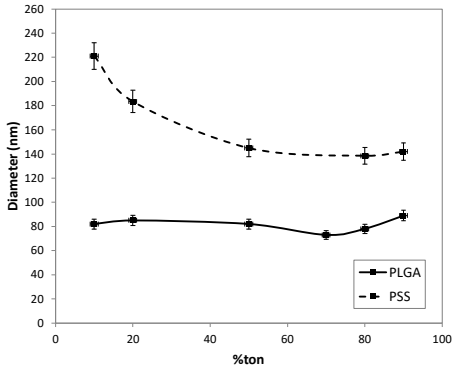

b)

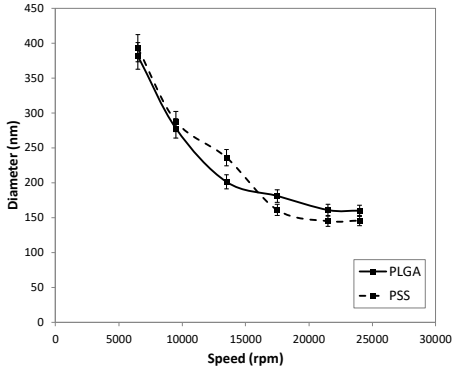

c)

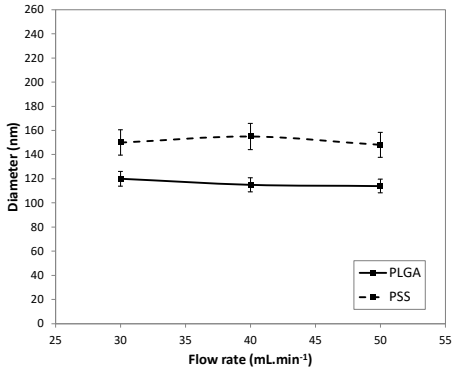

Figure 2. Evolution of PLGA and PSS NPs size regarding to the process mixing parameter for a) ultrasonicator (5 min), b) rotor-stator mixer (10 min) and c) elongational-flow micromixer (80 min). The C/D volume ratio was equal to 85/15 for all experiments.

In Figure 2.a, the minimum diameter values (140 nm and 80 nm for PSS and PLGA respectively) were obtained for a power amplitude between 50% and 90%. Moreover, for a cycle value higher than 70%, the colloïdal suspensions were not stable after three days: the NPs diameter increased and sedimentation was observed.
As observed in Figure 2.b, the rotational speed of the rotor-stator mixer highly impacted the PSS and PLGA NPs diameter that was divided by 3 when the speed was multiplied by 3. It also affected the solutions' stability that was stable for several hours at low speed (under 13,500 rpm) to two days at higher speed (≥ 17,500 rpm).
If for the two previous devices, the size of both PSS and PLGA NPS decreased while increasing the MP, observations in line with previous reported work for PLGA NPs,[33] the flow rate for the elongational-flow micromixer has virtually no influence on the polymeric NPs (Figure 2.c) over the range investigated (30 to 50 $mL.min^{-1}$). This complies well with a previous study[34] in which we reported the constant size of methyl methacrylate nanodroplets size past a given flow rate.
Interestingly, PSS NPs (dashed lines) were always bigger than PLGA NPs (solid lines), probably due to water penetration in these more hydrophilic NPs.
As reported in Table S1 and Table S3, the PDI values for PLGA NPs were below 0.2 for ultrasonicator and elongational-flow micromixer, proving the formation of monomodal nanoemulsions. However, the size dispersity was higher with the rotor-stator mixer (Table S2).

As a conclusion, the mixing parameters were fixed as described in Table 2.

III.1.2. Influence of the emulsification time

It is well-known that the emulsification time plays a crucial role on the particles' sizes.[34,35] This is why the influence of this parameter on the PSS and PLGA NPs diameter (Figure 3) as well as their PDI values (Table S4, Table S5) was investigated for the three different devices.

We first observed a PDI close to 0.2 (Table S4, Table S5) and a low variation of the NPs' diameter with the emulsification time for ultrasonication (Figure 3.a). Then, increasing the rotor-stator mixing or elongational-flow micromixing times decreased the PDI down to 0.17 and 0.15 respectively (for PLGA NPs) and down to 0.26 and 0.23 respectively (for PSS NPs). It also allowed the decrease of the average PLGA NPs size down to 144 nm (rotor-stator-mixer) and 104 nm (elongational-flow micromixer).
It was interesting to observe the increase in the PSS particles diameter past a threshold time of 80 min. This unusual behavior, mainly due to water penetration inside the PSS NPs, has already been observed and explained by our team in a previous study.[35]

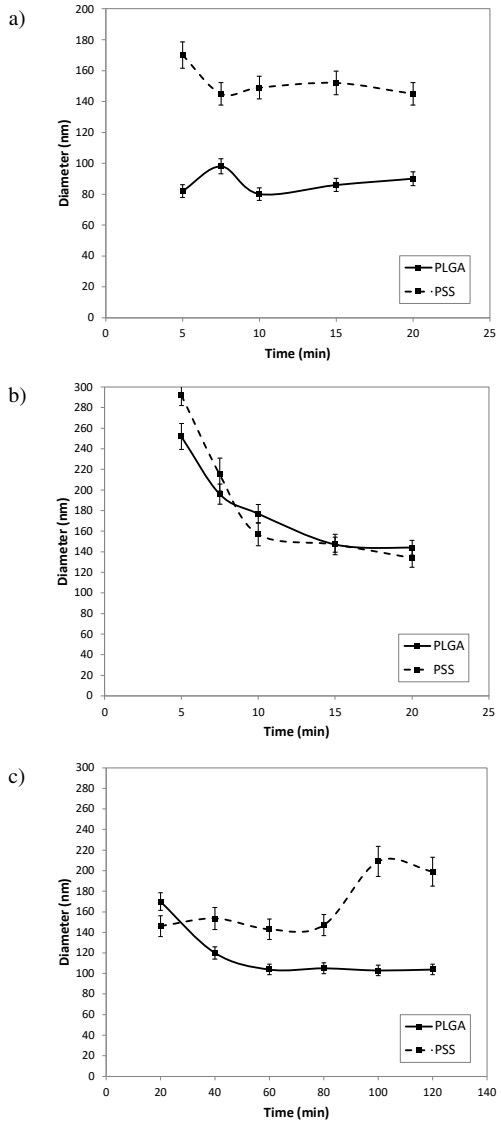

Figure 3. Evolution of PLGA and PSS NPs diameter regarding to the emulsification time for a) ultrasonicator, b) rotor-stator mixer and c) elongational-flow micromixer. The mixing parameter was kept constant (Table 2) and the C/D volume ratio was equal to 85/15 for all experiments.

So, we were now able to determine the optimum conditions to obtain nanoparticles with a low polydispersity index for each device (Table 3).

As observed in Figure 2 and Figure 3, PSS NPs (dashed lines) were always bigger than PLGA NPs (solid lines) due to water penetration inside PSS NPs since PSS was a more hydrophilic polymer than PLGA.[35] This systematic difference in size between small PLGA NPs and bigger PSS NPs was confirmed by cryo-TEM (Figure 4).

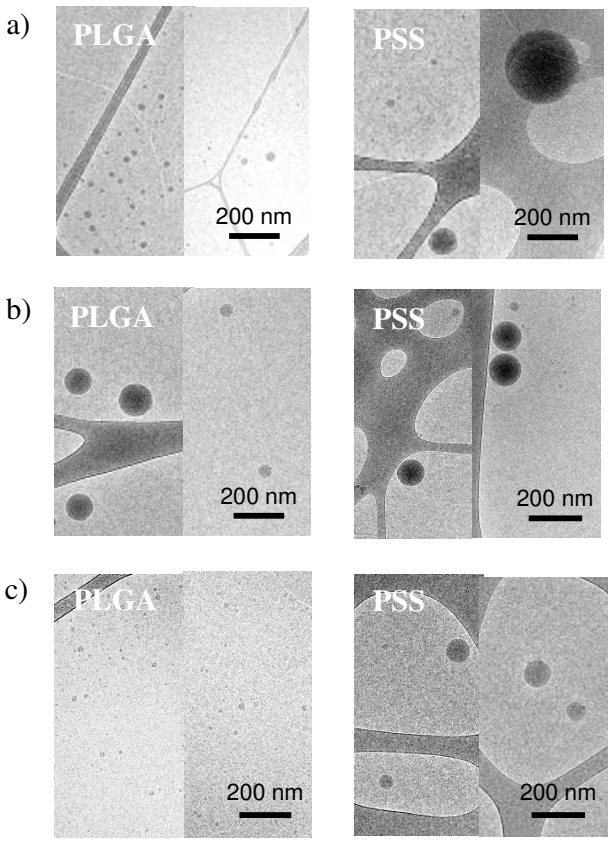

Figure 4. Cryo-TEM images of PLGA and PSS nanoparticles obtained by a) ultrasonication (50% of amplitude during 5 min), b) rotor-stator mixing (17,500 rpm during 10 min) and c) elongational-flow micromixing (30 mL.min^{-1} during 60 min). The C/D volume ratio was equal to 85/15 for all experiments.

III.1.3. Effect of the surfactant type

In this part, the mixing parameters (MP), the emulsification times and the C/D volume ratio were fixed as indicated in Table 3. The surfactant was either non-ionic (Pluronic® F-127) or anionic (SDS).

The SDS was an anionic surfactant, leading to more electronegative particles (zeta potential below -40 mV) than Pluronic® F-127 (zeta potential around -20 mV) for all the three devices.

Moreover, the anionic surfactant led to bigger, less stable PSS particles than the non-ionic surfactant (Table 4) because of electronic repulsion between SDS and PSS, both negatively charged. This also explained why few size differences were observed with both surfactants for PLGA NPs, PLGA being a neutral polymer.

III.1.4. Influence of continuous to dispersed phase volume ratio

For this study, the emulsifications occurred as described in Table 3 and the surfactant was non-ionic (Pluronic® F-127). We investigated the influence of C/D volume ratio, ranging from 90/10 to 70/30, on the NPs diameters (Figure 5).

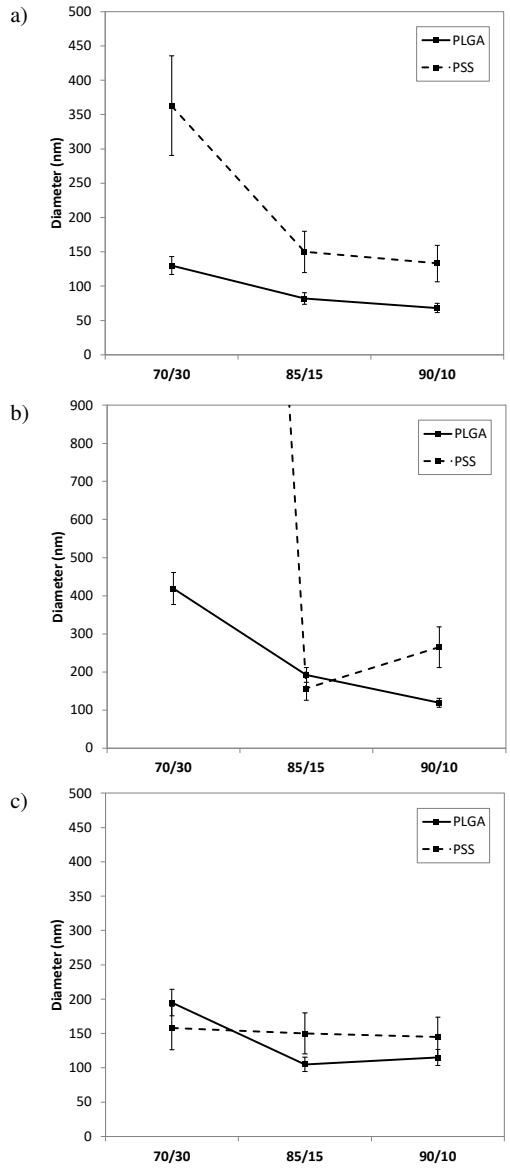

Figure 5. Evolution of the PLGA and PSS nanoparticles' size regarding to the C/D phase volume ratios. The NPs were obtained by a) ultrasonication (50% of amplitude during 5 min), b) rotor-stator mixing (17,500 rpm during 10 min) and c) elongational-flow micromixing (30 mL.min^{-1} during 60 min).

A larger amount of continuous phase led to smaller NPs for all the techniques. Indeed, the change in C/D volume ratio changed in particular the surfactant/organic phase weight ratio from 14% (C/D = 90/10) to 4% (C/D = 70/30), which has already been shown to be crucial in driving surfactant accumulation at the interface, particularly in the case of the sonication process.[36] The 70/30 phase volume ratio led to particles stable less than one day (phase separation). Moreover, particles' sizes were higher than 150 nm with ultrasonicator (Figure 5.a) and rotor-stator mixer (Figure 5.b) with this C/D volume ratio because of the high viscosity of the emulsions ($\eta_d/\eta_c >$ 4). Indeed, according to Grace' theory[37] viscosity ratios higher than 4 is the limiting value for these devices. This also explains why, when the C/D volume ratio decreased, the particles size increased less with the elongational-flow micromixer than with the other two devices.

Compared to PLGA NPs, a more drastic evolution of PSS particles size regarding to C/D volume ratios by ultrasonication and shear mixing than with elongational-flow micromixer was observed. A lower C/D volume ratio means a higher amount of PSS, leading to a more viscous solution and more electronic repulsion inside the par-

ticles. This is why it came out that poly(styrene sulfonate) was more marked by cavitation and shearing than elongational forces.

The optimal chemical parameters to obtain polymeric nanoparticles with the lowest size dispersity, determined by the last two studies, were summarized in Table 5.

III.2. Formation of polymeric Janus nanoparticles

In this second part, the possible formation of polymeric Janus nanoparticles (JNPs) with PSS and PLGA was investigated. In this purpose the mixing parameters (MP), the emulsification times, the surfactant type and the C/D volume ratio were fixed as indicated in Table 3 and Table 5.

III.2.1. Possible formation of Janus nanoparticles

Various nanosuspensions were elaborated with the three different processes by mixing PSS and PLGA in the dispersed phases using the optimal parameters (Table 3 and Table 5). In this part, the weight ratio of PSS to PLGA introduced in the dispersed solution "x" was equal to 1. Size measurements and cryo-TEM images were carried out in order to investigate the possible formation of JNPs.

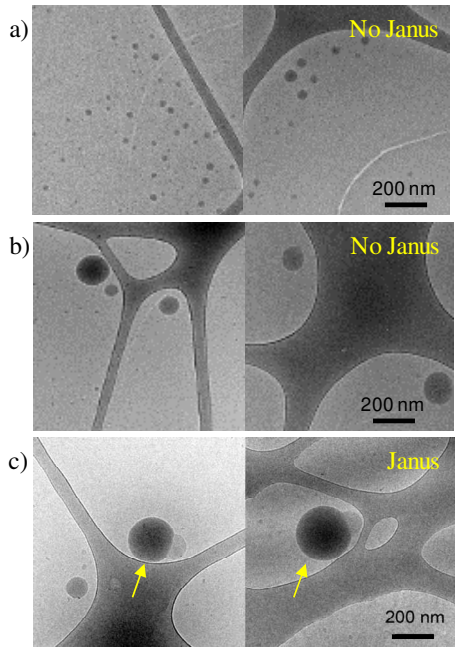

Figure 6. Cryo-TEM images of nanosuspensions obtained with a) ultrasonicator (50% of amplitude during 5 min), b) rotor-stator mixer (17,500 rpm during 10 min) and c) elongational-flow micromixer (30 mL.min^{-1} during 150 cycles).

For the ultrasonicator (Figure 6.a), one observed the formation of small circular NPs with two different uniform sizes (diameters around 60 nm and 40 nm), both with a low size polydispersity index (PDI around 0.12). The bimodal distribution was confirmed by DLS measurements (Figure S1.a). Considering the result obtained for the emulsification of individual polymers (Figure 4), this difference in size may suggest that the ultrasonicator did not allowed the production of Janus nanoparticles but led to the emulsification of the polymers (PLGA and PSS) separately. According to Figure 6.b and Figure S1.b, two populations of particles were also obtained with the rotor-stator mixer: 200 nm (PSS) and 70 nm (PLGA). These two devices are mainly reported in the literature for the production of micro- and nano-particles from monomers[38–40] but scarcely for polymers. Only two works could be found and reported larger size distributions of polymer NPs.[41,42] Therefore, these devices were not appropriated for the emulsification of viscous dispersed phases (here $\eta_d/\eta_c = 4.2$).[37]

Then, the production of monomodal (PDI = 0.17) Janus NPs with the elongational-flow micromixer was attended (Figure 6.c). On cryo-TEM images, the contrast between PLGA and PSS was related, as a first approximation, to the atomic number of the diffusing atoms. So, the two hemispheres observed for each particle were composed of the two different polymers. The monomodality of the nanoemulsions obtained with the elongational-flow micromixer was confirmed by DLS (Figure S1.c). Moreover, contrary to ultrasonication and rotor-stator mixing, the particles' size was constant for at least one month (Table S6).

This proved, for the first time, the ability of the elongational-flow micromixer to form composite polymeric Janus-like NPs in one-step from a polymer mixture, *i.e.* with viscous solutions. Therefore, and from now on, it will be the sole device employed for the production of Janus NPs.

III.2.2. Influence of the polymer amount on the nanoparticles' morphology

Operating the elongational-flow micromixer at a reciprocating flow rate of 30 mL.min^{-1} during 60 min, one investigated the influence of the weight ratio of PSS to PLGA introduced in the dispersed solution "x" (taken equal to 0.5, 1 or 2) on the variation of the NPs' size and morphology.

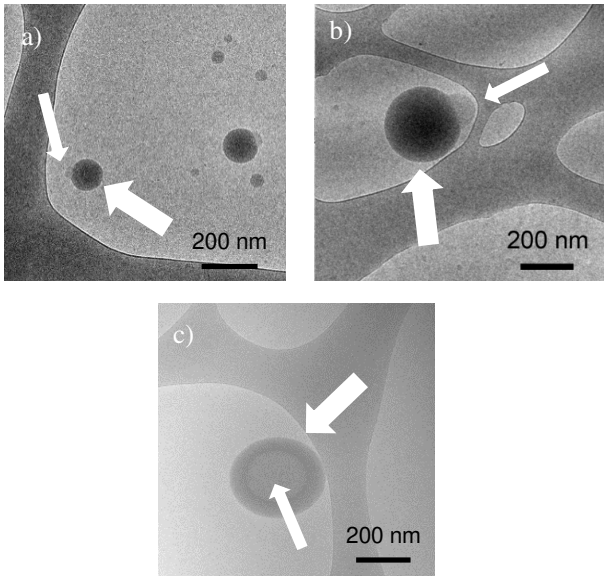

Figure 7. Cryo-TEM images of the nanosuspensions obtained when the weight ratio of PSS to PLGA introduced in the dispersed solution "x" was equal to a) 0.5, b) 1 and c) 2. For all these images, the emulsifications were realized with the elongational-flow micromixer at 30 mL.min^{-1} during 60 min.

In Table 6, increasing the weight ratio of PSS to PLGA in the dispersed solution (*i.e.* "x" value) increased the NPs size from 164 nm to 228 nm. However, the morphology was surprisingly not the same for all three "x" values. Interestingly, the ratio between the light area and the dark area was divided by two when the amount of PSS decreased from 1 (Figure 7.b) to 0.5 (Figure 7.a). So, PLGA-hemispheres were seen as dark grey zones (big arrows in Figure 7) and the PSS-hemispheres as lighter ones (thin arrows in Figure 7). However, when the PSS quantity was twice that of PLGA (Figure 7.c), a core-shell structure was observed instead of a Janus-like morphology. This can be explained by the possible charge-stabilization of the PSS core by the PLGA shell.

So, it was possible to tune the NPs morphology only by changing the polymer weight ratio introduced in the dispersed solution.

IV. CONCLUSION

Three different devices (ultrasonicator, rotor-stator mixer and elongational-flow micromixer) were used to produce nanoemulsions from biocompatible polymer(s) by emulsification-evaporation processes.
In a first part, this study demonstrated the possible one-step formation of polymeric nanoparticles with various size, ranging from 80 nm to 400 nm, depending on the device and their process parameters.
Then, the three devices allowed the production of nanoemulsions from a mixture of two immiscible polymers, poly(lactic-co-glycolic acid) (PLGA) and poly(styrene sulfonate) (PSS). However, the particles' chemical composition, diameter, size dispersity and morphology were different regarding the devices. Indeed, the ultrasonicator allowed the formation of bimodal nanosuspensions with small particles (60 nm PSS NPs and 40 nm PLGA NPs) and two populations of particles were also obtained with the rotor-stator mixer (200 nm PSS NPs and 70 nm PLGA NPs). This proved that these devices were not appropriated for the emulsification of a mixture of viscous polymeric solutions. However, the production of monomodal composite polymeric Janus NPs with the elongational-flow micromixer was observed.
Finally, the possible formation of different nanoparticles morphology (Janus and core-shell), depending on the relative quantity of the two polymers, was also demonstrated.

ACKNOWLEDGMENTS

The authors would like to thank Matéo Goetschy and Bérénice Baudin for their contribution. Mélanie Legros and Catherine Foussat are thanked for the access to the ICS characterization plateforms.

REFERENCES

(1) Poggi, E.; Ouvry, W.; Ernould, B.; Bourgeois, J.-P.; Chattopadhyay, S.; Prez, F. D.; Gohy, J.-F. Preparation of Janus Nanoparticles from Block Copolymer Thin Films Using Triazolinedione Chemistry. *RSC Adv.* **2017**, *7* (59), 37048–37054.
(2) Walther, A.; Müller, A. H. E. Janus Particles. *Soft Matter* **2008**, *4* (4), 663–668.
(3) Yánez-Sedeño, P.; Campuzano, S.; Pingarrón, J. M. Janus Particles for (Bio)Sensing. *Appl. Mater. Today* **2017**, *9*, 276–288.
(4) Jurado-Sánchez, B.; Escarpa, A. Janus Micromotors for Electrochemical Sensing and Biosensing Applications: A Review. *Electroanalysis* **2017**, *29* (1), 14–23.
(5) Yang, S.; Guo, F.; Kiraly, B.; Mao, X.; Lu, M.; W. Leong, K.; Jun Huang, T. Microfluidic Synthesis of Multifunctional Janus Particles for Biomedical Applications. *Lab. Chip* **2012**, *12* (12), 2097–2102.
(6) Wang, Y.-S.; Shao, D.; Zhang, L.; Zhang, X.-L.; Li, J.; Feng, J.; Xia, H.; Huo, Q.-S.; Dong, W.-F.; Sun, H.-B. Gold Nanorods-Silica Janus Nanoparticles for Theranostics. *Appl. Phys. Lett.* **2015**, *106* (17), 173705.
(7) Saini, S.; Kandasubramanian, B. Engineered Smart Textiles and Janus Microparticles for Diverse Functional Industrial Applications. *Polym.-Plast. Technol. Mater.* **2019**, *58* (3), 229–245.
(8) Zhang, L.; Zhu, Y. Dielectrophoresis of Janus Particles under High Frequency Ac-Electric Fields. *Appl. Phys. Lett.* **2010**, *96* (14), 141902.
(9) Gangwal, S.; Cayre, O. J.; Velev, O. D. Dielectrophoretic Assembly of Metallodielectric Janus Particles in AC Electric Fields. *Langmuir* **2008**, *24* (23), 13312–13320.
(10) Nisisako, T.; Torii, T.; Takahashi, T.; Takizawa, Y. Synthesis of Monodisperse Bicolored Janus Particles with Electrical Anisotropy Using a Microfluidic Co-Flow System. *Adv. Mater.* **2006**, *18* (9), 1152–1156.
(11) Ondarçuhu, T.; Fabre, P.; Raphaël, E.; Veyssié, M. Specific Properties of Amphiphilic Particles at Fluid Interfaces. *J. Phys.* **1990**, *51* (14), 1527–1536.
(12) Takei, H.; Shimizu, N. Gradient Sensitive Microscopic Probes Prepared by Gold Evaporation and Chemisorption on Latex Spheres. *Langmuir*, **1997**, *13* (7), 8165-1868.
(13) Himmelhaus, M.; Takei, H. Cap-shaped gold nanoparticles for an optical biosensor. *Sensors and Actuators B*. **2000**, *63*, 24-30.
(14) Cayre, O.; Paunov, V. N.; Velev, O. D. Fabrication of Dipolar Colloid Particles by Microcontact Printing. *Chem. Commun.* **2003**, *0* (18), 2296–2297.

(15) Koo, H. Y.; Yi, D. K.; Yoo, S. J.; Kim, D.-Y. A Snowman-like Array of Colloidal Dimers for Antireflecting Surfaces. *Adv. Mater.* **2004**, *16* (3), 274–277.
(16) Fujimoto, K.; Nakahama, K.; Shidara, M.; Kawaguchi, H. Preparation of Unsymmetrical Microspheres at the Interfaces. *Langmuir* **1999**, *15* (13), 4630–4635.
(17) Yin, Y.; Lu, Y.; Xia, Y. A Self-Assembly Approach to the Formation of Asymmetric Dimers from Monodispersed Spherical Colloids. *J. Am. Chem. Soc.* **2001**, *123* (4), 771–772.
(18) Mulvaney, P.; Giersig, M.; Ung, T.; Liz-Marzán, L. M. Direct Observation of Chemical Reactions in Silica-Coated Gold and Silver Nanoparticles. *Adv. Mater.* **1997**, *9* (7), 570–575.
(19) Wu, D.; Chew, J. W.; Honciuc, A. Polarity Reversal in Homologous Series of Surfactant-Free Janus Nanoparticles: Toward the Next Generation of Amphiphiles. *Langmuir* **2016**, *32* (25), 6376–6386.
(20) Yu, H.; Chen, M.; Rice, P.M.; Wang, S.X.; White, R.L.; Sun, S. Dumbbell-like Bifunctional Au−Fe_3O_4 Nanoparticles. *Nano Letters*. **2005**, *5* (2), 379-382.
(21) Perro, A.; Reculusa, S.; Ravaine, S.; Bourgeat-Lami, E.; Duguet, E. Design and synthesis of Janus micro- and nanoparticles. *J. Mater. Chem*. **2005**, *15*, 3745-3760.
(22) For more details, see http://www.gyriconmedia.com
(23) Photometrics©, Spinning Disk Confocal Microscopy, **2017**.
(24) Soppimath, K. S.; Aminabhavi, T. M.; Kulkarni, A. R.; Rudzinski, W. E. Biodegradable Polymeric Nanoparticles as Drug Delivery Devices. *J. Controlled Release* **2001**, *70* (1), 1–20.
(25) Jeon, H.-J.; Jeong, Y.-I.; Jang, M.-K.; Park, Y.-H.; Nah, J.-W. Effect of Solvent on the Preparation of Surfactant-Free Poly(D-Lactide-Co-Glycolide) Nanoparticles and Norfloxacin Release Characteristics. *Int. J. Pharm.* **2000**, *207* (1), 99–108.
(26) Allémann, E.; Leroux, J.-C.; Gurny, R. Polymeric Nano- and Microparticles for the Oral Delivery of Peptides and Peptidomimetics. *Adv. Drug Deliv. Rev.* **1998**, *34* (2), 171–189.
(27) Verma, A.; Stellacci, F. Effect of Surface Properties on Nanoparticle–Cell Interactions. *Small*. **2010**, *6* (1), 12-21.
(28) Davis, M. E.; Chen, Z. (Georgia); Shin, D. M. Nanoparticle Therapeutics: An Emerging Treatment Modality for Cancer. *Nanoscience and Technology*. **2009,** 239–250.
(29) Fröhlich, E. The Role of Surface Charge in Cellular Uptake and Cytotoxicity of Medical Nanoparticles. *Int. J. Nanomedicine* **2012**, *7*, 5577–5591.
(30) Masarudin, M. J.; Cutts, S. M.; Evison, B. J.; Phillips, D. R.; Pigram, P. J. Factors determining the stability, size distribution, and cellular accumulation of small, monodisperse chitosan nanoparticles as candidate vectors for anticancer drug delivery: application to the passive encapsulation of [^{14}C]-doxorubicin. *Nanotechnol. Sci. Appl*. **2015**, *8*, 67-80.
(31) Anton, N.; Bally, F.; Serra, C. A.; Ali, A.; Arntz, Y.; Mely, Y.; Zhao, M.; Marchioni, E.; Jakhmola, A.; Vandamme, T. F. A New Microfluidic Setup for Precise Control of the Polymer Nanoprecipitation Process and Lipophilic Drug Encapsulation. *Soft Matter.* **2012**, *8* (41), 10628.
(32) Ding, S.; Anton, N.; Vandamme, T. F.; Serra, C. A. Microfluidic Nanoprecipitation Systems for Preparing Pure Drug or Polymeric Drug Loaded Nanoparticles: An Overview. *Expert Opin. Drug Deliv.* **2016**, *13* (10), 1447–1460.
(33) Bilati, U.; Allémann, E.; Doelker, E. Sonication Parameters for the Preparation of Biodegradable Nanocapsulesof Controlled Size by the Double Emulsion Method. *Pharm. Dev. Techno.* **2003**, *8* (1), 1–9.
(34) Yu, W.; Serra, C. A.; Khan, I. U.; Ding, S.; Ibarra Gomez, r.; Bouquey, M.; Muller, R. Development of an Elongational-Flow Microprocess for the Production of Size-Controlled Nanoemulsions: Batch Operation. *Macromol. React. Eng*. **2017**, *11*, 1600024.
(35) Vauthier, M.; Serra, C. A. One-step Production of Polyelectrolyte Nanoparticles. *Polym. Internat.* **2021**, 70 (6), 860-865.
(36) Melanie, M.; Kosasih, F.Y.; Kasmara, H.; Malini, D.M.; Pnatarani, C.; Joni, I.M; Husodo, T.; Hermawan, W. Antifeedant Activity of Lantana Camara Nanosuspension prepared by Reverse Emulsion of Ethyl Acetate Active Fraction at Various Surfactant Organic-Phase Ratio. *Biocata. Agri. Biotech*. **2020**, *29*, 101805.

(37) Grace, H.P. Dispersion Phenomena in High Viscosity Immiscible Fluid Systems and Application of Static Mixers as Dispersion Devices in Such Systems. *Chem. Eng. Com*. **1982**, *14* (3-6), 225-277.
(38) Zheng, Z.; Zhang, X.; Carbo, D.; Clark, C.; Nathan, C.-A.; Lvov, Y. Sonication-Assisted Synthesis of Polyelectrolyte-Coated Curcumin Nanoparticles. *Langmuir*. **2010**, *26* (11), 7679-7681.
(39) Zanetti-Ramos, B. G.; Lemos-Senna, E.; Soldi, V.; Borsali, R.; Cloutet, E.; Cramail, H. Polyurethane Nanoparticles from a Natural Polyol via Miniemulsion Technique. *Polymer* **2006**, *47* (24), 8080–8087.
(40) Fonseca, L.B.; Nele, M.; Volpato, N.M.; Seiceira, R.C.; Pinto, J.C. Production of PMMA Nanoparticles Loaded with Praziquantel Through "In Situ" Miniemulsion Polymerization. *Macromol. React. Eng*. **2013**, *7* (1), 51-63.
(41) Mainardes, R. M.; Evangelista, R. C. PLGA Nanoparticles Containing Praziquantel: Effect of Formulation Variables on Size Distribution. *Int. J. Pharm.* **2005**, *290* (1), 137–144.
(42) Fang, R. H.; Aryal, S.; Hu, C.-M. J.; Zhang, L. Quick Synthesis of Lipid–Polymer Hybrid Nanoparticles with Low Polydispersity Using a Single-Step Sonication Method. *Langmuir*. **2010**, *26* (22), 16958-16962.

GRAPHICAL ABSTRACT

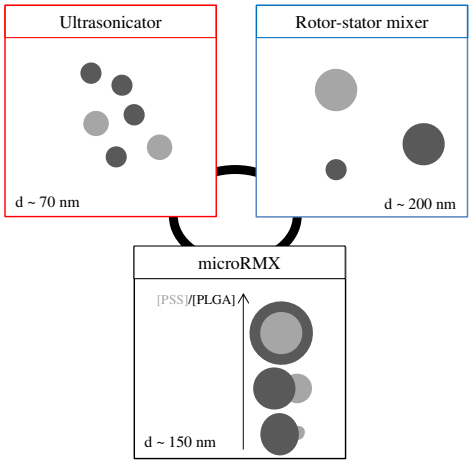

FIGURE CAPTIONS

Figure 1. Schematic illustration of the elongational-flow micromixing device.
Figure 2. Evolution of PLGA and PSS NPs size regarding to the process mixing parameter for a) ultrasonicator (5 min), b) rotor-stator mixer (10 min) and c) elongational-flow micromixer (80 min). The C/D volume ratio was equal to 85/15 for all experiments.
Figure 3. Evolution of PLGA and PSS NPs diameter regarding to the emulsification time for a) ultrasonicator, b) rotor-stator mixer and c) elongational-flow micromixer. The mixing parameter was kept constant (Table 2). The C/D volume ratio was equal to 85/15 for all experiments.
Figure 4. Cryo-TEM images of PLGA and PSS nanoparticles obtained by a) ultrasonication (50% of amplitude during 5 min), b) rotor-stator mixing (17,500 rpm during 10 min) and c) elongational-flow micromixing (30 mL.min^{-1} during 60 min). The C/D volume ratio was equal to 85/15 for all experiments.
Figure 5. Evolution of the PLGA and PSS nanoparticles' size regarding to the C/D phase volume ratios. The NPs were obtained by a) ultrasonication (50% of amplitude during 5 min), b) rotor-stator mixing (17,500 rpm during 10 min) and c) elongational-flow micromixing (30 mL.min^{-1} during 60 min).
Figure 6. Cryo-TEM images of nanosuspensions obtained with a) ultrasonicator (50% of amplitude during 5 min), b) rotor-stator mixer (17,500 rpm during 10 min) and c) elongational-flow micromixer (30 mL.min^{-1} during 150 cycles).

Figure 7. Cryo-TEM images of the nanosuspensions obtained when the weight ratio of PSS to PLGA introduced in the dispersed solution "x" was equal to a) 0.5, b) 1 and c) 2. For all these images, the emulsifications were realized with the elongational-flow micromixer at 30 mL.min^{-1} during 60 min.

TABLES

Table 1. Parameters used in order to produce PLGA or PSS nanoparticles with three different emulsification devices.

Process	MP	Time (min)	C/D
Ultrasonication	10 to 90% of amplitude (%t_{on})	5 to 20	70/30 to 90/10
Rotor-stator mixing	6,500 to 24,000 rpm	5 to 20	70/30 to 90/10
Elongational-flow micromixer	30 to 50 mL.min^{-1}	20 to 250	70/30 to 90/10

Table 2. Reference mixing parameters in order to obtain stable NPs with ultrasonicator, rotor-stator mixer and elongational-flow micromixer.

Process	Mixing parameter
Ultrasonication	Processing cycle = 50%
Rotor-stator mixing	17,500 rpm
Elongational-flow micromixer	30 mL.min^{-1}

Table 3. Reference conditions in order to obtain polymeric nanoemulsions with ultrasonicator, rotor-stator mixer and elongational-flow micromixer.

Process	Emulsification time	MP
Ultrasonication	5 min	Processing cycle = 50%
Rotor-stator mixing	10 min	17,500 rpm
Elongational-flow micromixer	60 min (150 cycles)	30 mL.min^{-1}

Table 4. Evolution of PLGA and PSS NPs size regarding to the type of surfactant for ultrasonicator (50% of amplitude during 5 min), rotor-stator mixer (17,500 rpm during 10 min) and elongational-flow micromixer (30 mL.min^{-1} during 60 min). P stands for Pluronic® F-127.

	PLGA		PSS	
	P	SDS	P	SDS
Ultrasonicator	82 ± 3	62 ± 21	150 ± 10	748 ± 132
Rotor-stator mixer	192 ± 9	226 ± 34	215 ± 26	305 ± 95
Elongational-flow micro-	104 ± 5	118 ± 24	143 ± 28	290 ± 32

mixer				

Table 5. Chemical conditions to obtain stable nanoparticles with PLGA and PSS with the three devices.

Surfactant	C/D volume ratio
Pluronic® F-127	85/15

Table 6. Evolution of the PLGA-PSS NPs size and the viscosity ratio η_d/η_c regarding to the weight ratio of PSS to PLGA "in the dispersed solution "x".

x	η_d/η_c	Diameter (nm)	PDI
0.5	4.1	164	0.10
1	4.2	156	0.13
2	5.2	228	0.24

One-step Elaboration of Janus Polymeric Nanoparticles: a Comparative Study of Different Emulsification Processes

Madeline Vauthier,†* Marc Schmutz†, Christophe Alexandre Serra†

† Université de Strasbourg, CNRS, Institut Charles Sadron UPR 22, F-67000 Strasbourg, France
Email: madeline.vauthier@ics-cnrs.unistra.fr, marc.schmutz@ics-cnrs.unistra.fr, ca.serra@unistra.fr

GRAPHICAL ABSTRACT